Archives of Biochemistry and Biophysics 491 (2009) 75–84

Contents lists available at ScienceDirect

Archives of Biochemistry and Biophysics

journal homepage: www.elsevier.com/locate/yabbi

Quinolinol and peptide inhibitors of zinc protease in botulinum neurotoxin A: Effects of zinc ion and peptides on inhibition ☆

Huiguo Lai [a], Minghao Feng [a], Virginia Roxas-Duncan [b], Sivanesan Dakshanamurthy [c], Leonard A. Smith [b,1], David C.H. Yang [a,*]

[a] Department of Chemistry, Georgetown University, Washington, DC 20057, USA
[b] Integrated Toxicology Division, US Army Medical Research Institute of Infectious Diseases, Fort Detrick, MD 21702, USA
[c] Lombardi Cancer Center, Georgetown University, Washington, DC 20057, USA

ARTICLE INFO

Article history:
Received 22 July 2009
and in revised form 12 September 2009
Available online 20 September 2009

Keywords:
Zinc protease
Inhibitor
Quinolinol
Peptide
Botulinum
Neurotoxin
Slow binding
Tight binding
Molecular modeling
Fluorescence titration

ABSTRACT

Quinolinol derivatives were found to be effective inhibitors of botulinum neurotoxin serotype A (BoNT/A). Studies of the inhibition and binding of 7-(phenyl(8-quinolinylamino)methyl)-8-quinolinol (QAQ) to the light chain domain (BoNT/A LC) showed that QAQ is a non-competitive inhibitor for the zinc protease activity. Binding and molecular modeling studies reveal that QAQ binds to a hydrophobic pocket near the active site. Its inhibitor effect does not involve the removal of zinc ion from the light chain. A 24-mer SNAP-25 peptide containing E183 to G206 with Q197C mutation (Peptide C) binds to BoNT/A LC with an unusually slow second order binding rate constant of 76.7 M^{-1} s^{-1}. QAQ binds to Zn^{2+}-free BoNT/A LC with a K_D of 0.67 μM and to Peptide C–BoNT/A LC complex with a K_D of 2.33 μM. The insights of the interactions of quinolinols and peptides with the zinc protease of BoNT/A should aid in the development of inhibitors of metalloproteases.

Introduction

Botulinum neurotoxins (BoNTs)[2] are the causative agents of botulism [1] and have been recognized as the most toxic substances known to man. BoNTs have found broad clinical applications in an increasing number of neurological diseases, such as dystonia, migraine headache, and others [2]. However, the potential nefarious misuse of these neurotoxins in a bioterrorist action could result in mass casualties requiring post-exposure therapy [3]. Effective medical countermeasures to treat victims after signs and symptoms of botulism have presented are limited, and therapies to target, inactivate and clear toxin from nerve cell are being actively sought worldwide.

The structures of BoNTs correlate well with their tripartite functional domains, which consist of a receptor binding domain, a translocation domain, and a zinc protease domain [4]. The associated zinc proteases, which form a light chain (LC), are highly specific to soluble *N*-ethylmaleimide-sensitive factor attachment protein receptors (SNARE), which mediate cellular and vesicular membrane fusion during neurotransmitter secretion [5]. Cleavage of the SNARE proteins by the LC blocks the release of acetylcholine from the presynapses, resulting in flaccid paralysis or botulism, and possibly death [6]. LCs have been a primary target for the development of therapeutics against botulism.

Several "unusual" properties of the zinc proteases in BoNTs have been discovered, such as their extraordinary substrate specificity [6], the extensive substrate–protease interactions in substrate recognition [7], the pivotal roles of amino acid residues distal from the active site in substrate binding and catalysis [8,9], and the PRIME and molten globular states during catalysis [10].

Recent progress in determining the three-dimensional structure of BoNTs has provided molecular insights about these neurotoxins and a computational basis for designing inhibitors based on the

☆ The work was supported by Defense Threat Reduction Agency/JSTO-CBD project No. 3.10037_07_RD_B.

* Corresponding author. Fax: +1 202 687 6209.
E-mail address: yangdc@georgetown.edu (D.C.H. Yang).
[1] Present address: Medical Countermeasures Technology, US Army Medical Research and Materiel Command, Fort Detrick, MD 21702, USA.

[2] *Abbreviations used:* BoNT/A LC, botulinum neurotoxin type A light chain; QAQ, 7-(phenyl(8-quinolinylamino)methyl)-8-quinolinol, NSC 84096; BAPQ, 7-((2-bromoanilino)(phenyl)methyl)-8-quinolinol, NSC 84086; CAPQ, 7-((4-chloroanilino)(phenyl)methyl)-8-quinolinol, NSC 84090; NAPQ, 7-((4-(hydroxy(oxido)amino)anilino)(phenyl)methyl)-8-quinolinol, NSC1010; Peptide C, Ac-EKADSNKTRIDEANCRATKMKLGSG-NH_2; Peptide C1, Ac-EKADSNKTRIDEANRATKMKLGSG-NH_2; K_D, apparent dissociation constant; K_i, inhibition constant; PAR, 4-(2-pyridylazo)resorcinol.

0003-9861/$ - see front matter © 2009 Elsevier Inc. All rights reserved.
doi:10.1016/j.abb.2009.09.008

Report Documentation Page

Form Approved
OMB No. 0704-0188

1. REPORT DATE	2. REPORT TYPE	3. DATES COVERED
20 SEP 2009	**N/A**	**-**

4. TITLE AND SUBTITLE	5a. CONTRACT NUMBER
Quinolinol and peptide inhibitors of zinc protease in botulinum neurotoxin A: effects of zinc ion and peptides on inhibition. Archives of Biochemistry and Biophysics 491:75-84	5b. GRANT NUMBER
	5c. PROGRAM ELEMENT NUMBER
6. AUTHOR(S)	5d. PROJECT NUMBER
Lai, H Feng, M Roxas-Duncan, V Dakshanamuthy, S Smith, LA Yang, DCH	5e. TASK NUMBER
	5f. WORK UNIT NUMBER
7. PERFORMING ORGANIZATION NAME(S) AND ADDRESS(ES)	8. PERFORMING ORGANIZATION REPORT NUMBER
United States Army Medical Research Institute of Infectious Diseases, Fort Detrick, MD	**TR-09-102**
9. SPONSORING/MONITORING AGENCY NAME(S) AND ADDRESS(ES)	10. SPONSOR/MONITOR'S ACRONYM(S)
	11. SPONSOR/MONITOR'S REPORT NUMBER(S)

12. DISTRIBUTION/AVAILABILITY STATEMENT
Approved for public release, distribution unlimited

13. SUPPLEMENTARY NOTES
The original document contains color images.

14. ABSTRACT
Recently, quinolinol derivatives were reported to inhibit the protease activity and reduce the toxicity of botulinum neurotoxin A. Our results show 7-(phenyl(8-quinolinylamino)methyl)-8-quinolinol (QAQ) bound to the light chain domain of botulinum neurotoxin A (BoNT/A LC) with an apparent dissociation constant (KD) of 0.02 M, inhibited the protease activity with an inhibition constant of 1.84 M, and exhibited a non-competitive inhibition pattern. QAQ was capable of binding to BoNT/A LC stripped of Zn2+ with a KD of 0.67 M. A 24-mer SNAP-25 peptide containing E183 to G206 with Q197C mutation (Peptide C) bound to BoNT/A LC with an unusually slow second order binding rate constant of 76.7 M-1sec-1. QAQ bound to the Peptide C-BoNT/A LC complex with a KD of 2.33 M. these results and molecular modeling suggest that QAQ inhibition was due to its binding to a hydrophobic site in BoNT/A LC and in the peptide-BoNT/A LC complex.

15. SUBJECT TERMS
Clostridium botulinum, neurotoxin, serotype A, quinolinol, peptide inhibitors, zinc

16. SECURITY CLASSIFICATION OF:			17. LIMITATION OF ABSTRACT	18. NUMBER OF PAGES	19a. NAME OF RESPONSIBLE PERSON
a. REPORT	b. ABSTRACT	c. THIS PAGE			
unclassified	**unclassified**	**unclassified**	**SAR**	**9**	

structure [4,11–15]. Recently, quinolinol-based compounds were reported to effectively inhibit the protease activity of both BoNT/A LC and BoNT/A holotoxin [16]. These results raised the likelihood that quinolinol derivatives can be therapeutic against BoNT. Quinolinols also showed anti-tumor activities [17,18]. Since the exact mechanism of inhibition by this class of compounds remains to be elucidated, we sought to analyze their inhibition and binding to BoNT/A LC. Preliminary studies revealed a disparate range of the concentrations for binding and inhibition suggesting that the inhibition may be affected by the high concentration of peptide substrate, the zinc ions in the buffer and at the active site of the zinc protease, the temperatures or pH of the buffers.

The interactions of zinc ion and protease inhibitors with the BoNTs appear to be complex. Holotoxin BoNT/A stripped of Zn^{2+} loses the protease activity but activity can be restored by exogenous Zn^{2+} [19]. The three-dimensional structures of the BoNT/A LC were essentially the same after stripping of Zn^{2+} [15,20]. A zinc chelator, bis(5-amidino-2-benzimidazolyl)methane (BABIM), binds to both the light chain and the holotoxin of BoNT serotype B, but very different inhibitory actions on the two forms of the protease were found [21,22]. Both small-molecule and peptide inhibitors bind to the Zn^{2+} at the active site of BoNT/A LC. Hydroxamates and the peptide inhibitor, CRATKML, bind directly to the Zn^{2+} with either two oxygens, or an oxygen and a sulfur, respectively. The inhibitory binding mode of the peptide inhibitor CRATKML evidently involves the coordination of Zn^{2+} by the cysteine in CRATKML as determined by X-ray crystallography [20,23]. Elucidation of the roles of zinc ions and the peptides on the binding and inhibition of BoNT/A LC by quinolinols should provide insights for the development of inhibitors of BoNTs as well as zinc proteases in general [24].

In this paper, we examined the inhibition and binding of BoNT/A LC with the quinolinol derivatives and peptide inhibitors by enzyme kinetics, fluorescence studies, removal of Zn^{2+} from the BoNT/A LC active site, and molecular modeling. Here we show that the effective quinolinol inhibitors bind to Zn^{2+}-free BoNT/A LC and peptide–BoNT/A LC complexes. The results suggest that the inhibitory structure corresponds to the QAQ binding mode to the peptide–BoNT/A LC complex. The modes of QAQ inhibition have significant implications for their use and provide a rationalization for their different effects in various assays.

Materials and methods

Materials

QAQ, BAPQ, CAPQ and NAPQ were custom-synthesized by GLSynthesis (Worchester, MA), with identity confirmed by mass spectrometry and the purity by HPLC of greater than 98%. Peptides including Ac-CRATKML-NH_2, Peptide C (Ac-EKADSNKTRIDEAN-CRATKMLGSG-NH_2) and Peptide C1 (Ac-EKADSNKTRIDEANAR-ATKMLGSG-NH_2) were prepared and purified by C S Bio Co., Menlo Park, CA. The purity was greater than 95% based on the HPLC chromatograms. SNAPtide (o-Abz/Dnp) was purchased from List Biological Laboratory and was used according to manufacturer's instructions unless otherwise specified. Truncated BoNT/A LC (1–425) was a kind gift of J. Barbieri (Medical College of Wisconsin) and was used for fluorescence titration and for microtiter protease assays using full-length SNAP-25 as the substrate [25]. BoNT/A LC fused with SUMO was constructed [26] and will be presented elsewhere. Test compounds were stored at −20 °C until use.

Fluorescence measurements

All fluorescence measurements were made in 10 mM sodium phosphate (pH 7.4), 150 mM NaCl, and 10 μM zinc acetate at 25 °C using SPEX Fluomax and 0.4 × 0.4 × 3 cm microcuvettes unless otherwise specified. The intrinsic fluorescence of the light chain was determined at 323 nm with an excitation wavelength of 280 nm. Samples with an absorbance at 280 nm greater than 0.02 were corrected for the inner filter effect. The intrinsic fluorescence of the light chain exhibited two exponential decays and slowly stabilized by 60 min to 70% of the initial fluorescence after diluting the stock solution to the above buffer. The fluorescence decays consisted of two single exponentials and the rate constants were independent of the protein concentration. The fluorescence decreases were consistent with the dissociation of BoNT/A LC dimers to monomers or conformational changes upon the dilution of BoNT/A LC. However, the exact cause was not clear. All light chain samples were thus pre-incubated in the above buffer for 60 min at 25 °C before measuring fluorescence.

Zn^{2+} removal and Zn^{2+} assay

To remove the Zn^{2+} in the light chain, the protein was incubated in a buffer containing 10 mM EDTA and 150 mM sodium phosphate (pH 7.5), and then dialyzed against the same buffer at 4 °C overnight, and then re-dialyzed at 4 °C against 2500 volumes of 150 mM sodium phosphate (pH 7.5) pretreated chelex-100 with two changes overnight. The resulting light chain stripped of Zn^{2+} was stored at 4 °C and contained no detectable Zn^{2+} at 8 μM light chain as determined by the 4-(2-pyridylazo)resorcinol (PAR) indicator assay. The PAR Zn^{2+} assay was carried out as described [27]. Briefly, protein samples were incubated in 6 M guanidinium chloride, 30 mM sodium phosphate (pH 7.5), and 100 μM PAR at 25 °C for 15 min. The absorbance of PAR in complex with Zn^{2+} at 500 nm was determined. The amounts of Zn^{2+} in the protein samples were obtained by interpolating onto a standard curve of zinc acetate with PAR in the same buffer.

Determination of the dissociation constants

The fluorescence of BoNT/A LC (0.2 μM) in 250 μl of 10 mM sodium phosphate (pH 7.4) and 10 μM zinc acetate at 323 nm (λ_{ex} at 280 nm) was monitored in the presence of various concentrations of quinolinol derivatives in a microcuvette (0.4 × 0.4 × 3 cm) by adding 1 μl aliquots of inhibitor in the same buffer at an increment in a range of 0.02–0.2 μM unless otherwise specified. The changes in the fluorescence (ΔF) and the extent of binding (α) were used to calculate K_D based on the fluorescence quenching of the BoNT/A LC (Eq. (1)) as follows:

$$\alpha = \frac{\Delta F}{\Delta F_{max}} = \frac{F_0 - F}{F_0 - F_{max}} = \frac{x_b}{E_0} = \frac{(E_0 + x_0 + K) - [(E_0 + x_0 + K)^2 - 4E_0x_0]^{1/2}}{2E_0} \quad (1)$$

where F_0, F, and F_{max} are the BoNT/A LC intrinsic fluorescence intensities with excitation at 280 nm and emission at 323 nm, in the absence of the inhibitor, in the presence of limiting concentrations of inhibitor, and in the presence of a saturating concentration of inhibitor, respectively. X_0 is the total concentration of inhibitor, X_b is the concentration of the BoNT/A LC-bound inhibitor, and E_0 is the total BoNT/A LC concentration. The solution of the quadratic equation was obtained using the equilibrium constant equation [28]. The monomeric light chain was found to have one binding site at saturating concentrations of the inhibitors. Sigmaplot was used for hyperbolic and exponential fitting and data analysis is reported as ±standard error.

Determination of Michaelis–Menten kinetic constants

SNAPtide was used as the substrate for analyzing the solution kinetics of protease inhibition. SNAPtide protease assays were carried out in 10 mM potassium phosphate, pH 7.4, 10 μM zinc acetate, and 150 mM NaCl at 25 °C unless otherwise specified. SNAPtide was incubated with and without the inhibitor at room temperature in the above buffer in the presence of varying concentrations of SNAPtide. The reactions were initiated by the addition of BoNT/A LC. The protease activity was monitored by the initial rates of the increase of fluorescence intensity at 420 nm with an excitation wavelength of 320 nm. All reactions were carried out to less than 5% completion. The results were analyzed using Sigmaplot and the Michaelis–Menten equation to obtain the Michaelis–Menten constants and maximal velocities.

Modeling using quantum mechanics and molecular mechanics (QM/MM)

The X-ray crystal structure of the catalytically active light chain of BoNT/A (PDB: 1XTG) without the bound endopeptide, was used in this study. Inconsistencies between the PDB format and the LC residue library translation to atomic potential types were corrected manually. The LC was minimized using the DISCOVER (Accelrys, San Diego, CA) program's CFF91 force field with distance-dependent dielectrics.

The inhibitors were retrieved as 2D structures from the NCI database and were geometrically optimized using standard MMFF94 force field, with a 0.001 kcal/mol energy gradient convergence criterion employing Gasteiger charges. Full geometric optimization and charges were calculated by the MP2/6-311G** approach using Gaussian03. Docking simulations were performed using FlexX [29]. FlexX treats metal/ligand interactions as ionic interactions. The best conformation in the active site was selected irrespective of the scoring function from the top 120 conformations generated by FlexX. The following criteria were used: (1) the distance cut-off was set to 2.5 Å between the ligand interacting atom and the catalytic Zn^{2+}, (2) the FlexX docked conformations are based on the maximum possible interactions (hydrophobic, Zn coordination, electrostatic, H-bond, etc.) with the target catalytic active site, and 3) the agreement docking approach [30]. The Zn^{2+}-coordinated histidine residues were treated as the neutral form with the hydrogen on ND1, while other histidine residues used the default option with hydrogen on NE2. Glutamate and aspartate residues were treated as the charged form as the default.

The best docked geometries were further selected as follows: a modified CFF91 was used to allow for the inclusion of the Zn^{2+}, its ligands, and their nearest closest neighbors. The parameters for these new potential types were estimated from quantum mechanical calculations on a Zn^{2+}-coordinated system. During the refinement, the Zn^{2+} and residues coordinating it were fixed in their original coordinates. The cut-off for non-bonded interaction energies was set to ∞ (i.e., no cut-off). The structures were gradually relaxed, to avoid unrealistic movements of the enzyme caused by computational artifacts. The dielectric constant was set at 4 to account for the dielectric shielding found in proteins. Each minimization was carried out in two steps by first using the steepest descent minimization for 200 cycles, and subsequently using conjugate gradient minimization with a gradient criterion of 0.01 kcal/mol. All atoms within 15 Å of the inhibitor were allowed to relax during the minimization. The minimized complexes were subjected to MD simulations using the DISCOVER module of Insight II (DISCOVER, Accelrys Inc., San Diego). MD simulations consisted of an initial equilibration of 5 picoseconds (ps) followed by 100 ps dynamics at 300 K. The final structure of the complex at the end of the MD simulation was subjected to 5000 steps of the steepest descent energy minimization followed by conjugate gradient energy minimization. For all of the above calculations, a distance-dependent dielectric constant and non-bonded distance cut-off of 20 Å were used.

The inhibitor–enzyme complexes were further simulated using the QM/MM approach. By adopting Eq. (2) to describe the binding energy of BoNT with an inhibitor, the binding energy ΔE can be calculated as:

$$\Delta E_{QM/MM} = \langle E^{complex}_{QM/MM} \rangle - \langle E^{ligand}_{QM/MM} \rangle - \langle E^{receptor}_{QM/MM} \rangle \quad (2)$$

where the energies $E^{complex}_{QM/MM}$, $E^{ligand}_{QM/MM}$ and $E^{receptor}_{QM/MM}$ correspond to the enzyme–inhibitor complex, the free inhibitor and the free enzyme, respectively. The QM region consisted of residues within 7 Å of the Zn^{2+}, the entire inhibitor, and the Zn^{2+}. The rest of the protein was considered the MM region. The QM and MM regions interact by electrostatic interactions between MM point charges and the QM wave function, and by van der Waals interactions between QM and MM atoms [31]. This partitioning yielded a model, described by a quantum mechanical method, embedded into an environment described by a force field. The amide groups (HN–CO) were included in the definition of the quantum mechanical region. For the QM and MM parts, the Density Functional Theory (DFT) B3LYP method and CFF91 force field were used, respectively. All charges in the MM region were treated using the CFF91 force field. The B3LYP method is an accurate DFT method and provides better geometries and energies than those from correlated *ab initio* methods for the first-row transition metal complexes [32]. The 6-311++G** basis set was used in the interface region between the QM and MM region and the diffuse functions are recommended when using the transition metals. All the hybrid QM/MM calculations were performed using the Turbomole and Discover software incorporated in the InsightII/QuanteMM program (Accelrys Inc., San Diego, CA).

Results

Tight binding of quinolinol derivatives to BoNT/A LC

The structures of the selected quinolinol inhibitors used in this study are shown in Fig. 1. The interactions of these quinolinol derivatives with BoNT/A LC were first characterized by their K_Ds. The intrinsic fluorescence of BoNT/A LC was effectively quenched by the four quinolinol derivatives at mid-nanomolar concentrations (data not shown). The tight binding between BoNT/A LC and the quinolinol derivatives was analyzed using Eq. (1) to include corrections for the change of concentrations of unbound ligand (see Materials and methods). The K_Ds for the BoNT/A LC complex with QAQ, BAPQ, CAPQ and NAPQ were 0.020 ± 0.0013, 0.142 ± 0.021, 0.127 ± 0.029 and 0.114 ± 0.022 μM, respectively (data not shown). QAQ was the focus of the subsequent studies due to its tight binding to BoNT/A LC. Quinolinol is known to chelate Zn^{2+} with a K_D of 10^{-8} M [33]. The BoNT/A LC binding study was carried out in the presence of 10 μM zinc acetate to alleviate the chelation of Zn^{2+} from the active site of BoNT/A LC by quinolinols. Similar K_Ds (18.6 ± 4.1 nM for QAQ) were obtained using a buffer without Zn^{2+}. In the presence of 10 mM zinc acetate, which creates a large excess of Zn^{2+}, the affinity of QAQ to BoNT/A LC was reduced but the binding of the quinolinols remained tight with a K_D of 214 ± 16 nM (data not shown). Thus, the binding results were consistent with the tight binding of the quinolinol derivatives to BoNT/A LC and in part through chelation.

Effects of temperature and pH

We sought to analyze the effects of varying experimental parameters such as temperature and pH on the inhibitor binding.

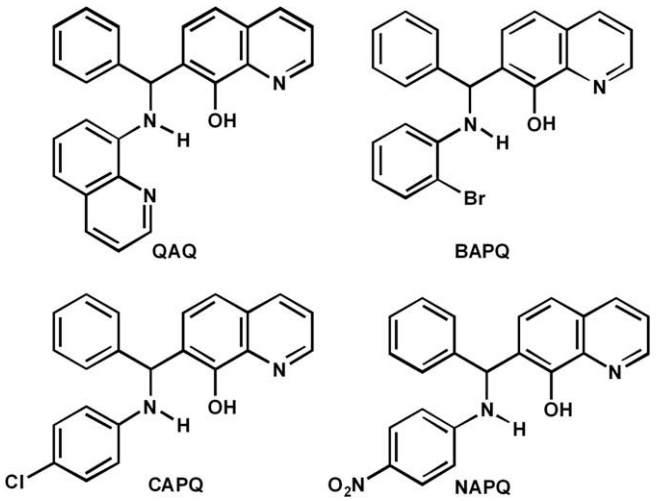

Fig. 1. Structural formula of the four quinolinol derivatives used in the present study. QAQ (7-(phenyl(8-quinolinylamino)methyl)-8-quinolinol, NSC 84096); BAPQ (7-((2-bromoanilino)(phenyl)methyl)-8-quinolinol, NSC 84086); CAPQ (7-((4-chloroanilino)(phenyl)methyl)-8-quinolinol, NSC 84090); NAPQ (7-((4-(hydroxy(oxido)amino)anilino)(phenyl)methyl)-8-quinolinol, NSC1010). Shown here are the abbreviated IUPAC names and the NSC code numbers at the NCI data base (http://129.43.27.140/ncidb2/).

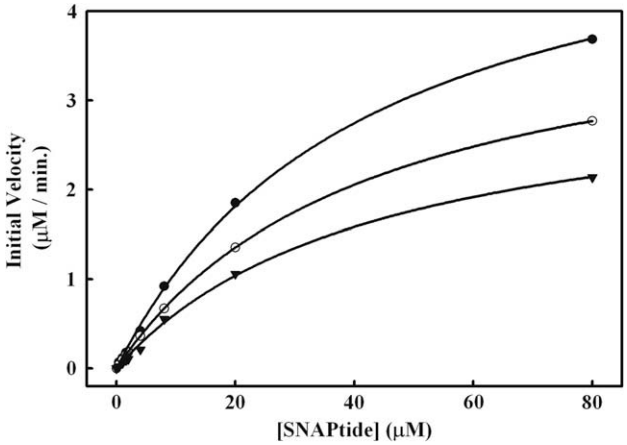

Fig. 2. Inhibition of BoNT/A LC protease activity by QAQ. Initial reaction rates of the SNAPtide cleavage catalyzed by 0.2 μM BoNT/A LC in 10 mM phosphate (pH 7.4), 150 mM NaCl and 10 μM zinc acetate at 25 °C were determined at changing fixed concentrations of QAQ at 0 (solid circle), 1 μM (open circle) and 5 μM (solid triangle) and varying concentrations of SNAPtide. The reactions were initiated by the addition of BoNT/A LC and the fluorescence intensity at 420 nm was monitored with an excitation wavelength at 320 nm. Reactions were less than 5% completion in all cases to maintain valid steady-state measurements. The solid lines are fitted lines using the Michaelis–Menten equation. See text for the values of the Michaelis–Menten constants, maximal velocities and standard errors.

The K_D of QAQ to BoNT/A LC increased from 0.016 ± 0.0056 μM at 25 °C to 0.023 ± 0.0014 μM and 0.071 ± 0.022 μM at 37 °C and 42 °C, respectively (data not shown). The decreased affinity of the BoNT/A LC corresponded to a decrease in the entropy of 135 J mol^{-1} K^{-1} of the QAQ binding. The large negative binding entropy is consistent with the involvement of hydrophobic interactions in the QAQ binding to the BoNT/A LC.

We next examined the effects of changing pH of the buffer on the binding of QAQ to BoNT/A LC. When the pH was reduced to 5, the affinity of QAQ to BoNT/A LC decreased slightly. The K_Ds at pH 5 were 0.04 ± 0.016, 0.096 ± 0.032 and 0.113 ± 0.048 μM at 25, 37 and 42 °C, respectively (data not shown). The slight decrease in affinity could be partially attributed to protonation of the quinolinol amino group at the lower pH. The lack of a major change in the K_D in relation to temperature and pH suggested that high temperature and low pH were unlikely to drastically affect the affinity of QAQ to BoNT/A LC.

Non-competitive inhibition of BoNT/A LC by QAQ

The steady-state kinetics of QAQ inhibition of BoNT/A LC protease activity were examined using the FRET protease assay with SNAPtide as the substrate in the presence of excess zinc acetate (10 μM). Varying concentrations of SNAPtide at changing fixed concentrations of QAQ in steady-state kinetic analysis gave nearly identical Michaelis–Menten constants of 42.3 ± 2.42, 42.7 ± 2.27 and 43.7 ± 3.76 μM SNAPtide at 0, 1 and 5 μM QAQ, respectively (Fig. 2). Under the same conditions, the maximal velocities decreased from 5.64 to 4.2 μM/min and 3.3 μM/min for 0, 1 and 5 μM QAQ, respectively. Since QAQ affected the maximal velocity of SNAPtide cleavage catalyzed by BoNT/A LC without affecting the Michaelis–Menten constant for SNAPtide, QAQ appears to be a non-competitive inhibitor of BoNT/A LC. The corresponding inhibition constant, K_i, for QAQ was 1.84 ± 0.12 μM.

The inhibition of BoNT/A LC by QAQ was also examined by the microtiter assay using full-length SNAP-25 [25]. The IC_{50} of QAQ was 0.93 ± 0.032 and 1.21 ± 0.034 μM in the presence of 10 and 250 μM zinc acetate, respectively.

Comparison of the K_D from fluorescence titrations of QAQ and BoNT/A LC with the effective QAQ concentrations for protease inhibition of BoNT/A LC unexpectedly showed differences of nearly two orders-of-magnitude. These results are not likely to be due to the experimental parameters of the binding and protease assays, such as temperatures (25 vs. 37 °C), since binding studies performed at various temperatures and pHs showed relatively small changes. The differences are most likely due to the different peptide concentrations (0 μM in binding studies vs. 10–200 μM in protease assays). These results suggest that the interactions involved in QAQ binding and in peptide binding may be important in understanding the mechanism of QAQ inhibition.

Roles of Zn^{2+} chelation in quinolinol inhibition

Because quinolinols are known to chelate divalent cations [33], the potential roles of chelation on the inhibition of BoNT/A LC protease activity were examined. The Zn^{2+} in the light chain is required for catalysis. Whether QAQ inhibited the light chain protease activity by removing Zn^{2+} from the light chain was examined as follows. Zn^{2+} in the light chain was first stripped by incubating with 10 mM EDTA followed by dialysis against Chelex-100 pretreated buffer. The stripping of Zn^{2+} was confirmed using the chromogenic PAR assay [27]. The light chain stripped of Zn^{2+} that lost the protease activity as monitored by real-time SNAPtide protease assay was instantaneously restored to 80% activity by the

Table 1
Reactivation of BoNT/A LC stripped of Zn^{2+}.

	Rate of SNAPtide cleavage[a]	Zn^{2+} stoichiometry[b]
BoNT/A LC in Zn^{2+}-free buffer	100	1.1
BoNT/A LC in 10 μM Zn^{2+}	115	
Zn^{2+}-free BoNT/A LC in Zn^{2+}-free buffer	0	ND[c]
Zn^{2+}-free BoNT/A LC in 10 μM Zn^{2+}	80	

[a] Protease activity of BoNT/A LC (0.2 μM) was determined by the SNAPtide FRET assay. The rates are shown as that relative to native BoNT/A LC in zinc free buffer and defined as 100.

[b] The Zn^{2+} content was determined by the PAR chromogenic assay. The concentration of native BoNT/A LC was 8 μM in 150 mM sodium phosphate (pH 7.5). The concentration of Zn^{2+}-free BoNT/A LC was 8 μM in Chelex-100 pretreated 150 mM sodium phosphate (pH 7.5) (see Materials and methods for details).

[c] Not detectable.

addition of zinc acetate (Table 1). Zn^{2+}-free BoNT/A LC (0.2 μM) was titrated with QAQ in Chelex-100 pretreated buffer containing 10 mM phosphate (pH 7.4), 150 mM NaCl. Binding of QAQ was monitored by the change in the intrinsic fluorescent intensity of Zn^{2+}-free BoNT/A LC induced by QAQ. The K_D determined for QAQ binding to Zn^{2+}-free BoNT/A LC was 0.67 ± 0.05 μM (data not shown). QAQ inhibited the protease activity of light chain with a K_i of 1.84 μM in the presence of a large excess of Zn^{2+} relative to that of QAQ used. The fact that the value of K_i is similar to that of K_D for QAQ binding to the Zn^{2+}-free light chain suggests that QAQ inhibition of the light chain protease activity depends at least in part on the Zn^{2+}-independent binding pocket. The QAQ inhibition of the protease activity was unlikely due to the removal of Zn^{2+} by QAQ from the light chain since the protease activity could be immediately restored as the Zn^{2+} returns to the light chain in the presence of excess Zn^{2+}.

Binding of Peptide C to BoNT/A LC

To further probe the interaction of QAQ with BoNT/A LC, synthetic peptide with the amino acid sequence corresponding to SNAP-25 residues E183 to G206 but with a Q198C mutation, AcE-KADSNKTRIDEANCRATKMLGSG-NH_2, abbreviated as Peptide C, was synthesized. The C197 in Peptide C was incorporated to prevent Peptide C from being cleaved by BoNT/A LC. The binding of synthetic Peptide C was first examined using fluorescence titration by monitoring the fluorescence intensity of BoNT/A LC upon addition of varying concentrations of Peptide C. The K_D of Peptide C–BoNT/A LC complex in PBS containing 10 μM zinc acetate was found to be 0.04 ± 0.01 μM as determined by monitoring the intrinsic fluorescence of BoNT/A LC. The IC_{50} of the Peptide C in PBS containing 10 μ M zinc acetate was 3.4 ± 0.27 μM as determined by the SNAPtide protease assay.

BoNT/A LC binding of QAQ in the presence of Peptide C

The binding of QAQ to BoNT/A LC at indicated fixed concentrations of Peptide C was analyzed by monitoring the intrinsic fluorescence of BoNT/A LC. The K_Ds of QAQ to BoNT/A LC were 0.020 ± 0.0054, 0.066 ± 0.011, 0.124 ± 0.018, and 0.224 ± 0.034 μM in the presence of 0, 0.2, 1, and 2 μM Peptide C, respectively (data not shown). Thus, the affinity of QAQ to BoNT/A LC was moderately affected by Peptide C.

The interactions of QAQ with BoNT/A LC were next examined in the presence of higher concentrations of Peptide C (>10 μM). Fig. 3 shows the QAQ binding curves with BoNT/A LC in the presence of 20, 40, and 60 μM Peptide C as determined by monitoring the intrinsic fluorescence of BoNT/A LC. The binding curves evidently consisted of two distinct phases. The binding at low concentrations of QAQ quenched the intrinsic fluorescence of BoNT/A LC and had a similar affinity as that observed in the absence of Peptide C, while the second phase showed fluorescence enhancement. The biphasic binding of QAQ in the presence of high concentrations of Peptide C suggested that the second phase of binding occurred at a much slower rate than the first phase such that second phase binding could not occur simultaneously with the first phase binding to give a smooth titration curve. Peptide C appears to bind slowly to BoNT/A LC and the fluorescence enhancement was due to the binding of QAQ to the complex of BoNT/A LC and Peptide C. These findings led us to analyze the time courses for the kinetics of Peptide C binding to BoNT/A LC.

Slow binding of Peptide C to BoNT/A LC

The time courses for the Peptide C binding to BoNT/A LC were determined by monitoring the time dependent changes in the intrinsic fluorescence quenching immediately after incubating with Peptide C (Fig. 4). Binding of the Peptide C to BoNT/A LC was slow and followed pseudo-first order reaction time courses in the presence of a large excess of Peptide C in comparison to BoNT/A LC. The second order rate constant for Peptide C binding to BoNT/A LC was determined from the observed pseudo-first order rate constants at varying concentrations of Peptide C and found to be 76.7 M^{-1} s^{-1}.

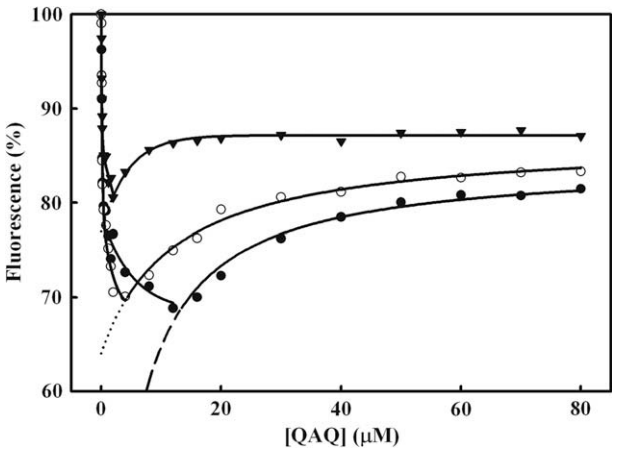

Fig. 3. Fluorescence titration of BoNT/A LC with QAQ in the presence of Peptide C. The intrinsic fluorescence of BoNT/A LC (0.2 μM) in 10 mM phosphate (pH 7.4), 150 mM NaCl, 10 μM zinc acetate was monitored with the addition of varying concentrations of QAQ in the presence of 20 μM (●), 40 μM (○) and 60 μM (▼) Peptide C. The fluorescence intensity was measured at 323 nm with the excitation wavelength at 280 nm. The changes of the fluorescence intensity with the concentrations of the inhibitors were analyzed as described in Material and methods. Solid lines are fitted curves of the K_Ds shown in the text using Eq. (1). The solid lines were fitted lines to the two phases of fluorescence changes using Eq. (1).

Binding of QAQ to the BoNT/A LC–Peptide C complex

BoNT/A LC was pre-incubated with varying concentrations of Peptide C for 60 min at 25 °C to allow the formation of the Peptide C–BoNT/A LC complex. The Peptide C–BoNT/A LC complex remained intact based on the dissociation rate for the complex,

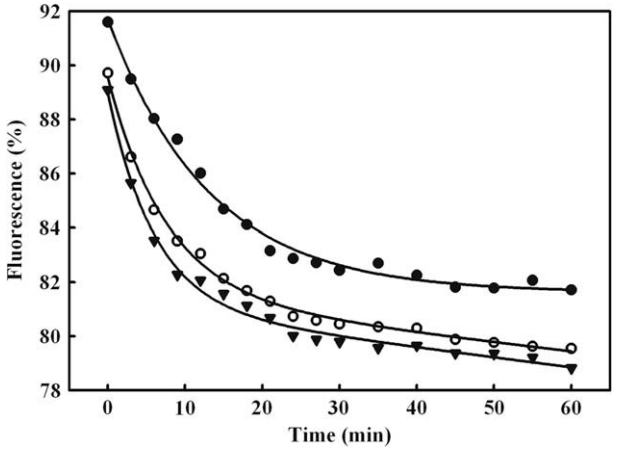

Fig. 4. The time courses of the BoNT/A LC binding of Peptide C. The fluorescence intensity of the intrinsic fluorescence of BoNT/A LC (0.2 μM) in 10 mM phosphate (pH 7.4), 150 mM NaCl, and 10 μM zinc acetate was monitored immediately after the addition of Peptide C to final concentrations of Peptide C to (●) 1.0 μM; (○) 5.0 μM; (▼) 20.0 μM at 25 °C. The time courses were fitted according to first order reaction kinetics and provided pseudo-first order rate constants of 0.077 ± 0.012, 0.103 ± 0.011 and 0.167 ± 0.016 min^{-1}, at 1, 5 and 20 μM Peptide C, respectively.

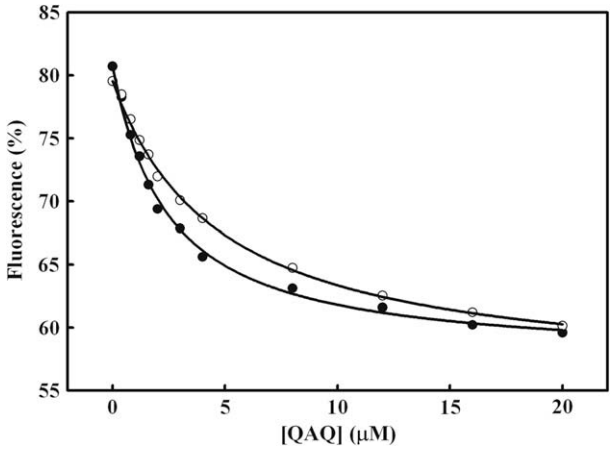

Fig. 5. Binding of QAQ with the Peptide C–BoNT/A LC complex. BoNT/A LC (0.2 μM) was pre-incubated with Peptide C at (●) 1.0 μM and (○) 5.0 μM in 10 mM phosphate (pH 7.4), 150 mM NaCl, 10 μM zinc acetate for 60 min at 25 °C to form the Peptide C–BoNT/A LC complex. The fluorescence intensity of the complex was then monitored after the addition of varying concentrations of QAQ. The titration curves were analyzed using Eq. (1) to obtain the K_Ds. The K_Ds for QAQ in the presence of 1.0 and 5.0 μM Peptide C were 2.33 ± 0.14 and 4.63 ± 0.24 μM, respectively. The solid lines represent the fitted lines.

which was calculated from the K_D and the observed second order rate constant for Peptide C binding to BoNT/A LC. When the Peptide C–BoNT/A LC complex was titrated with QAQ, BoNT/A LC showed additional quenching as monitored by the intrinsic fluorescence of BoNT/A LC. As shown in Fig. 5, the K_Ds of QAQ to BoNT/A LC were 2.33 ± 0.14 and 4.63 ± 0.24 μM in the presence of 1 and 5 μM Peptide C, respectively.

The K_Ds thus obtained correlated with the IC_{50} of QAQ as determined by the HPLC protease assay for BoNT/A LC, suggesting that the binding mode of QAQ to BoNT/A LC in the presence of Peptide C more likely resembles its inhibition mode.

BoNT/A LC binding to Peptide C1

An analog of Peptide C (Peptide C1) with an alanine substituting the cysteine in Peptide C was then synthesized to analyze the effect of cysteine on the binding of QAQ to BoNT/A LC. Unlike cysteine in Peptide C, the alanine in Peptide C1 is unable to coordinate the Zn^{2+} in BoNT/A LC. The time courses of the Peptide C1 binding to BoNT/A LC are shown in Fig. 6A. At 1 μM Peptide C1, BoNT/A LC exhibited a monophasic first order time course with a pseudo-first order rate constant of 0.128 min^{-1}. At higher concentrations of Peptide C1, binding to BoNT/A LC showed two exponential biphasic time courses. The fast phase had pseudo-first order rate constants of 0.263 and 0.515 min^{-1} at 5.0 and 20.0 μM Peptide C1, respectively. The second order rate constant for the Peptide C1 binding to BoNT/A LC was 323 M^{-1} s^{-1} for the fast phase. The slow phase binding corresponded to pseudo-first order rate constants of 0.0936 and 0.0681 min^{-1} at 5.0 and 20.0 μM Peptide C1, respectively. The slow phase in the time courses for Peptide C1 binding to BoNT/A LC could be due to non-specific binding to secondary binding sites in BoNT/A LC or to secondary slow conformational changes of the Peptide C1–BoNT/A LC complex.

Binding of QAQ to the Peptide C1–BoNT/A LC complex

The binding of QAQ to the Peptide C1–BoNT/A LC complex was next examined. BoNT/A LC and Peptide C1 were pre-incubated for 60 min to form the Peptide C1–BoNT/A LC complex. Addition of varying concentrations of QAQ to the Peptide C1–BoNT/A LC complex resulted in additional quenching of the intrinsic fluorescence of BoNT/A LC (Fig. 6B). The K_Ds for QAQ binding to the Peptide C1–BoNT/A LC complex thus obtained were 1.89 ± 0.18 and 3.13 ± 0.40 μM at 1 and 5 μM Peptide C1, respectively. The similar K_Ds of QAQ binding to the Peptide C– or Peptide C1–BoNT/A LC were also obtained. These results suggest that the binding of QAQ to BoNT/A LC was little affected by the substitution of cysteine to alanine in Peptide C.

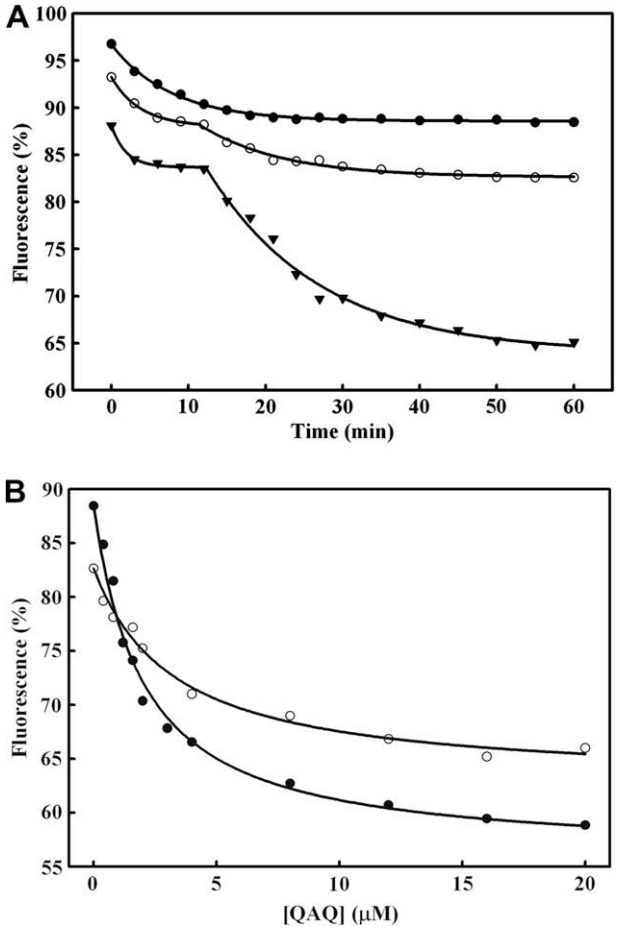

Fig. 6. Interactions of BoNT/A LC with Peptide C1 and QAQ. (A) The time courses of the binding of Peptide C1 to BoNT/A LC The fluorescence intensity of the intrinsic fluorescence of BoNT/A LC (0.2 μM) in 10 mM phosphate (pH 7.4), 150 mM NaCl, 10 μM zinc acetate was monitored immediately after the addition of Peptide C1 to final concentrations of Peptide C1 to (●) 1.0 μM; (○) 5.0 μM; (▼) 20.0 μM at 25 °C. The time courses were fitted according to first order reaction kinetics and provided pseudo-first order rate constants of 0.13 ± 0.0052, 0.26 ± 0.025 and 0.51 ± 0.096 min^{-1}, at 1, 5 and 20 μM Peptide C1, respectively, for the fast phase of the biphasic time courses. The pseudo-first order rate constants for the second phases were 0.0936 and 0.0681 min^{-1} at 5.0 and 20.0 μM Peptide C1, respectively, for the slow phase of the biphasic time course at high concentrations of Peptide C1. The solid lines represent the fitted lines to single exponential time courses. (B) QAQ binding to the complex of BoNT/A LC and Peptide C1. BoNT/A LC (0.2 μM) was first pre-incubated with 5.0 μM Peptide C1 for 1 h at 25 °C to form the Peptide C1–BoNT/A LC complex. The fluorescence intensity of the complex was monitored after additions of varying concentrations of QAQ. The K_Ds for QAQ to BoNT/A LC were 1.88 ± 0.18 and 3.13 ± 0.40 μM in the presence of 1.0 (●) and 5.0 μM (○) Peptide C1, respectively. The solid lines are fitted curves using Eq. (1).

Binding mode of QAQ to BoNT/A LC

Fig. 7A shows the geometrically minimized binding model of QAQ obtained using the QM/MM method. This compound has very few rotatable bonds, hence it possesses restricted conformations that reduce the number of potential binding modes it may assume

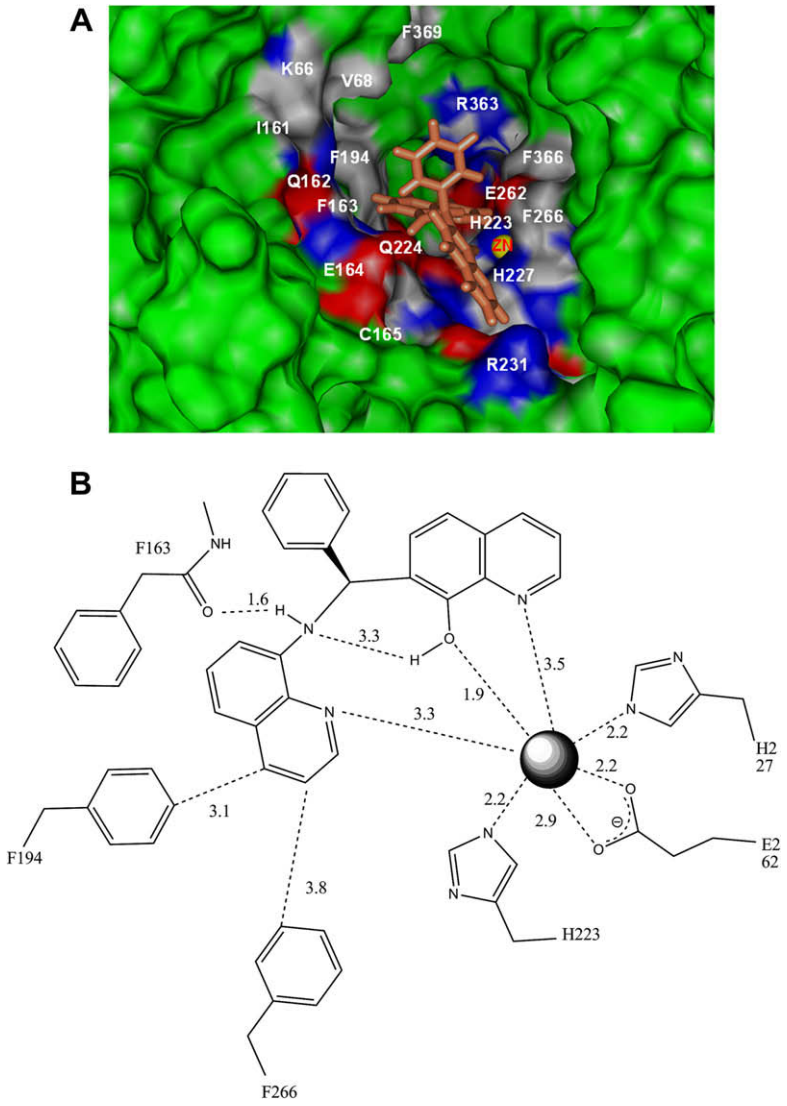

Fig. 7. The binding mode of QAQ with BoNT/A LC from QM/MM simulations. (A) The molecular surface of the BoNT/A LC, created with the MOLCAD module of Sybyl 7.0 is represented by green with active site interacting residues shown by atom color. QAQ is shown as stick model and atoms are colored in coral. The catalytic Zn^{2+} is represented as a sphere (colored yellow). (B) Schematic presentation of the QAQ–BoNT/A LC complex. Zn^{2+} coordination, hydrogen bonding and hydrophobic interactions are depicted for the QAQ–BoNT/A LC complex. (For interpretation of the references to colour in this figure legend, the reader is referred to the web version of this article.)

in the enzyme's catalytic active site. As seen in Fig. 7A, the oxygen and nitrogen atoms of the 8-hydroxyquinoline are within the distance of 2.0 and 3.5 Å, respectively, from the catalytic Zn^{2+}. The hydroxyl moiety may displace the water molecule that is used during catalysis. The benzene ring of the ligand points toward a hydrophobic pocket formed by the aromatic residues F366 and F369, and the non-polar residues L256 and V68. The cationic center of K66 is located near the centroid normal of the pi system of the benzene ring but the ring plane is slightly twisted. However, the distance between the ε-amino group and the aromatic ring system is within 4.5 Å and thus falls within the cation-π contact distance [34] with the ring. The quinoline moiety that is buried deep in the pocket forms a stacking interaction with H223, and is surrounded by hydrophobic ring clusters such as F163, F194, and F266. The 8-hydroxyquinoline ring is stacked with H227, makes hydrophobic contacts with the carbon atoms of E164, and cation-π contacts with R231. The cation-π interactions could make important contributions to increased affinity [35]. Fig. 7B shows the binding mode of QAQ to BoNT/A LC with the distances to neighboring residues and Zn^{2+} and with the hydrophobic pocket binding the benzene ring.

Binding mode of QAQ to the SNAP-25–BoNT/A LC complex

The binding mode of QAQ to the SNAP-25–BoNT/A LC complex (PDB 1XTG) was similarly examined. As shown in Fig. 8A and B, the active site pocket in BoNT/A LC bound to SNAP-25 can accommodate QAQ. The QAQ quinolinol ring N and hydroxyl O are 3.5 and 5.7 Å, respectively, away from the Zn^{2+} in the active site and could not chelate the Zn^{2+}. Quinolinol exocyclic N is hydrogen bonded to the carboxyl O of Asp370. Phe 163 and Phe 194 form a hydrophobic wall surrounding the quinolinol and quinoline rings. QAQ was thus deep in the hydrophobic pocket near the active site of BoNT/A LC in the presence of SNAP-25.

Discussion

QAQ is the first small-molecule inhibitor of BoNT/A that was found to be effective in inhibiting the protease activity of BoNT/A as determined by biochemical assay and in reducing the toxicity of BoNT/A by cell- and tissue-based assays [16]. In this study, we set out to elucidate the mechanism of QAQ binding to BoNT/A LC

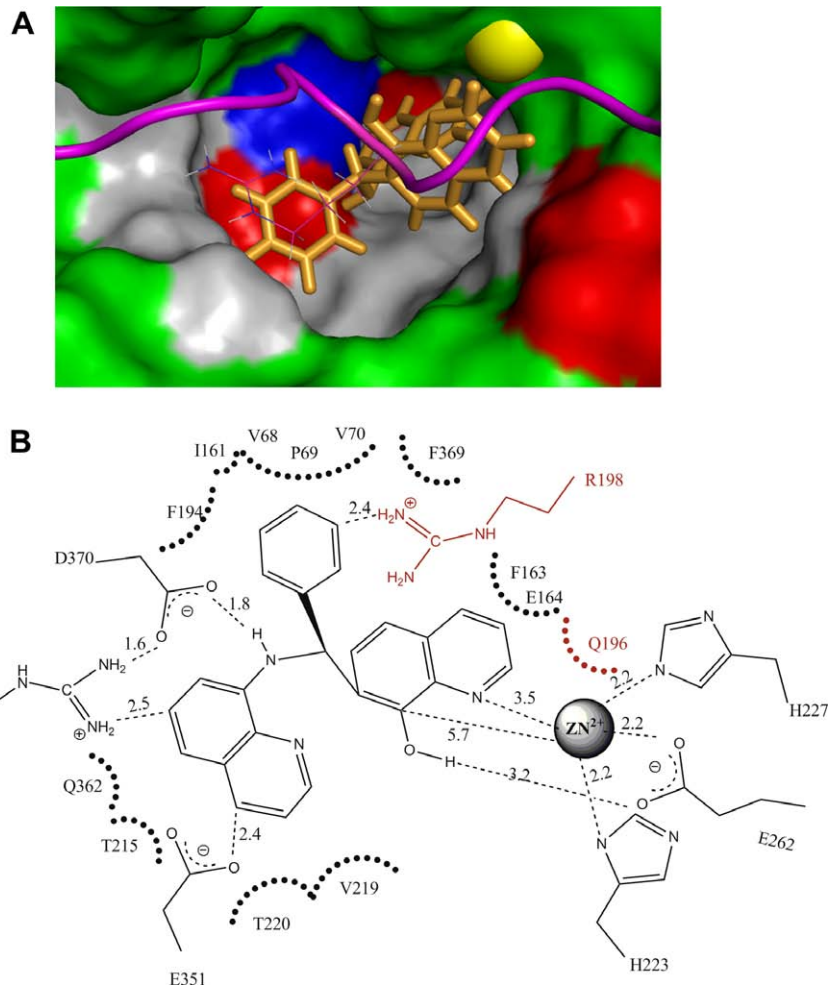

Fig. 8. The binding mode of QAQ to the SNAP-25 (141–204)–BoNT/A LC complex. (A) The binding pocket is labeled with amino acid residues from BoNT/A LC (gray for hydrophobic, blue for basic and red for acidic residues), the Zn^{2+} in yellow, the SNAP-25 in purple, and QAQ in beige. (B) Schematic presentation of the QAQ binding mode with the SNAP-25 (141–204)–BoNT/A LC complex. (For interpretation of the references to colour in this figure legend, the reader is referred to the web version of this article.)

and QAQ inhibition of the protease activity, and also to establish the actions of these inhibitors under various conditions. QAQ bound to native BoNT/A LC with a K_D of 0.02 μM as determined by monitoring the intrinsic fluorescence of BoNT/A LC, and that its affinity was reduced to a K_D of 0.214 μM at high concentrations of Zn^{2+} but was not significantly affected by temperature and pH. QAQ inhibited the protease activity with a K_D of 1.84 μM. Removal of Zn^{2+} from BoNT/A LC reduced the QAQ affinity to a K_D of 0.67 μM. Thus, the QAQ affinity to Zn^{2+}-free BoNT/A LC correlated with the K_i of QAQ as determined by the SNAPtide assay. Binding of BoNT/A LC at 0.02 μM QAQ likely involves chelation of Zn^{2+} in the active site of BoNT/A LC, but did not inhibit the protease activity. QAQ inhibition of the protease activity could not be due to the removal of Zn^{2+} from the protease since the inhibition was observed with Zn^{2+} (10 μM) in excess of QAQ and Zn^{2+} re-binding to Zn^{2+}-free BoNT/A LC was instantaneous. Moreover, the inhibition was observed at concentrations much higher than the K_D (~0.01 μM) expected for quinolinol chelation to Zn^{2+} [33]. The binding of QAQ to Zn^{2+}-free BoNT/A LC demonstrated the presence of the Zn^{2+}-independent QAQ binding site in BoNT/A LC.

The three-dimensional structures of the BoNT/A LC are the same with or without Zn^{2+} [15,20]. It appears that QAQ binds to a hydrophobic pocket near the active site of Zn^{2+}-free BoNT/A LC (K_D of 0.67 μM), and chelates Zn^{2+} at the active site of BoNT/A LC in the presence of zinc (K_D of 0.02 μM).

The steady-state enzyme kinetic analysis of the QAQ inhibition of BoNT/A LC protease activity was consistent with non-competitive inhibition based on the results that the catalytic constant was reduced with increasing concentrations of QAQ and the Michaelis–Menten constant did not change (Fig. 2). The non-competitive inhibition pattern suggests the QAQ binds to the enzyme–substrate complex and the free form of enzyme. The observation that QAQ bound to Zn^{2+}-free BoNT/A LC with a K_D of 0.67 μM and to the Peptide C–BoNT/A LC complex with a K_D of 2.33 μM was in agreement with the K_i of 1.84 μM. The difference between the K_D and the K_i could be due to the differences in the types of assays.

Peptide C is able to bind to BoNT/A LC and inhibits BoNT/A LC protease activity. The very slow binding of long peptides such as Peptide C to BoNT/A LC was first observed based on the unusual biphasic QAQ binding to BoNT/A LC in the presence of Peptide C (Fig. 3). The slow binding of Peptide C to BoNT/A LC was in contrast to the short peptide inhibitor CRATKML, which did not show slow binding (Feng and Yang, unpublished data). Based on the observed second order rate constant (k_{on}) of 76 $M^{-1}\,s^{-1}$ and the K_D of 24.9 nM for Peptide C binding to BoNT/A LC, the dissociation rate constant of the Peptide C–BoNT/A LC complex was calculated to be $1.91 \times 10^{-6}\,s^{-1}$. The peptide–BoNT/A LC complexes would not dissociate in days based on the observed second order binding rate constant and K_D. Such slow dissociation allows a new approach in

developing antagonists of BoNT/A similar to the very tight binding of naturally occurring protease inhibitors such as soybean trypsin inhibitor to trypsin.

The K_D of QAQ to BoNT/A LC in the presence of Peptide C, which contains a cysteine, was similar to that in the presence of C1, which replaces the cysteine with an alanine, suggesting that QAQ coordination to the Zn^{2+} in BoNT/A LC did not play a major role in the QAQ binding to the peptide–BoNT/A LC complexes. The coordination of the cysteine in CRATKML with the Zn^{2+} in BoNT/A LC has been shown by X-ray crystallography [20]. The cysteine in Peptide C, which contains CRATKML, is also likely to be coordinated to the Zn^{2+} in BoNT/A LC. However, a potent peptidomimetic inhibitor in complex with BoNT/A LC adopts a helical instead of the extended conformation of bound SNAP-25 [36]. Either conformation that Peptides C and C1 adopt will reduce the QAQ access to the Zn^{2+} in the active site. The present results suggest that Zn^{2+} in BoNT/A LC plays a minor role in the QAQ binding to the peptide–BoNT/A LC complexes.

The exact nature of the mechanism for the slow binding of long peptides is yet to be determined. Since comparable slow binding was observed for the binding of both Peptides C and C1 to BoNT/A LC, the slow binding was at least in part likely due to the extensive interactions of peptides with BoNT/A LC. Long peptides could have more extensive interactions with BoNT/A LC than shorter peptides. The binding of long peptides to BoNT/A LC could necessitate BoNT/A LC undergo conformational changes or it could require the selection of specific conformers of the long peptides from large conformation ensembles before productive binding to BoNT/A LC can occur. The later scenario is plausible considering a potent peptidomimetic inhibitor adopts a very different conformation from that of SNAP-25 [36]. Whether or not the release of natural substrates and products from the BoNT/A holotoxin resembles the release of Peptides C and C1 from BoNT/A LC is not known. The slow release of long peptides observed in the present study raises the possibility that this event is one of the factors contributing to the prolonged action of BoNT/A *in vivo*.

Molecular modeling of the QAQ–BoNT/A LC complexes in the absence and in the presence of SNAP-25 provided two plausible binding modes. The binding mode in the absence of the peptide showed that QAQ may be coordinated by the Zn^{2+} in BoNT/A LC (Fig. 7), while QAQ may not interact strongly with the Zn^{2+} in the BoNT/A LC–peptide complex (Fig. 8). The varying extent of Zn^{2+} interaction with QAQ in the two different binding modes likely contributed to the large differences between the QAQ K_Ds with BoNT/A LC in the absence (0.017 μM) and in the presence (4.63 μM) of long peptides. The presence of Peptides C or C1 evidently affected the interactions of QAQ with BoNT/A LC. The K_Ds of QAQ binding to BoNT/A LC in the presence of Peptide C (4.63 μM) or C1 (3.13 μM) were much greater than the K_Ds in the absence of the peptides (0.02 μM). It is likely a direct consequence of the exclusion of QAQ chelation of zinc at the active site by the binding of the peptide to the active site of BoNT/A LC. This is consistent with the observed difference between the K_D of the BoNT/A LC (0.02 μM)) and that of the Zn^{2+}-free BoNT/A LC (0.67 μM). Because the observed K_D of QAQ in the presence of Peptide C (4.63 μM) or C1 (3.13 μM) closely correlated with the K_i and IC_{50} of QAQ as determined by three different assays, including SNAPtide assays (K_i of 2.84 μM), SNAP-25 microtiter assays (IC_{50} of 1.21 μM), and HPLC assays (IC_{50} of 1.6–4.7 μM from [16]), the binding mode of QAQ in the presence of SNAP-25 (Fig. 8) likely resembles the *inhibitory* binding mode. Because QAQ reduced the catalytic efficiency of BoNT/A LC as shown by the reduced maximal velocity, QAQ likely inhibits the formation of the transition state intermediate. The presence of two binding modes for an inhibitor of BoNT/A LC provides new insights towards protease-inhibitor design. The results suggest that the peptide substrate may play an important role in the action of the inhibitor and thus in the development of inhibitors.

Conclusions

The present studies demonstrate QAQ evidently is able to bind to Zn^{2+}-free BoNT/A LC and the peptide–BoNT/A LC complexes. The QAQ inhibition of the protease activity was not due to chelation or removal of zinc ion from BoNT/A LC. QAQ inhibited the zinc protease activity via a non-competitive inhibition mechanism. QAQ binds at a hydrophobic pocket of BoNT/A LC. Molecular modeling studies of the QAQ–BoNT/A LC complex in the absence of the peptide showed that QAQ may be coordinated by the Zn^{2+} in BoNT/A LC, while in the presence of the peptide, QAQ may not interact strongly with the Zn^{2+} in the BoNT/A LC–peptide complex. Long peptides such as Peptide C and C1 were found to bind very slowly and tightly to BoNT/A LC. The slow and tight binding of the long peptides could conceivably allow a new approach for the peptide inhibitor design. The insights of the interactions of quinolinols and peptides with the zinc protease of BoNT/A should aid in the development of inhibitors of metalloproteases in general.

Disclaimer

Opinions, interpretations, conclusions, and recommendations are those of the authors and are not necessarily endorsed by the US Army.

Acknowledgments

The authors thank J. Barbieri (Medical College of Wisconsin) for the truncated BoNT/A LC (1–425). We acknowledge the National Cancer Institute for allocation of computing time, and staff support at the Advanced Biomedical Computing Center, National Cancer Institute, MD, USA.

References

[1] C. Montecucco, G. Schiavo, Q. Rev. Biophys. 28 (1995) 423–472.
[2] K. Turton, J.A. Chaddock, K.R. Acharya, Trends Biochem. Sci. 27 (2002) 552–558.
[3] L.M. Wein, Y. Liu, Proc. Natl. Acad. Sci. USA 102 (2005) 9984–9989.
[4] D.B. Lacy, W. Tepp, A.C. Cohen, B.R. DasGupta, R.C. Stevens, Nat. Struct. Biol. 5 (1998) 898–902.
[5] T.C. Sudhof, J.E. Rothman, Science 323 (2009) 474–477.
[6] G. Schiavo, A. Santucci, B.R. Dasgupta, P.P. Mehta, J. Jontes, F. Benfenati, M.C. Wilson, C. Montecucco, FEBS Lett. 335 (1993) 99–103.
[7] M.A. Breidenbach, A.T. Brunger, Nature 432 (2004) 925–929.
[8] S. Chen, J.T. Barbieri, J. Biol. Chem. 281 (2006) 10906–10911.
[9] S. Chen, J.T. Barbieri, J. Biol. Chem. 282 (2007) 25540–25547.
[10] R. Kukreja, B. Singh, J. Biol. Chem. 280 (2005) 39346–39352.
[11] B. Segelke, M. Knapp, S. Kadkhodayan, R. Balhorn, B. Rupp, Proc. Natl. Acad. Sci. USA 101 (2004) 6888–6893.
[12] J.W. Arndt, W. Yu, F. Bi, R.C. Stevens, Biochemistry 44 (2005) 9574–9580.
[13] R. Agarwal, S. Eswaramoorthy, D. Kumaran, T. Binz, S. Swaminathan, Biochemistry 43 (2004) 6637–6644.
[14] R. Agarwal, T. Binz, S. Swaminathan, Biochemistry 44 (2005) 11758–11765.
[15] Z. Fu, S. Chen, M.R. Baldwin, G.E. Boldt, A. Crawford, K.D. Janda, J.T. Barbieri, J.J. Kim, Biochemistry 45 (2006) 8903–8911.
[16] V. Roxas-Duncan, I. Enyedy, V.A. Montgomery, V.S. Eccard, M.A. Carrington, H. Lai, N. Gul, D.C. Yang, L.A. Smith, Antimicrob. Agents Chemother. 53 (2009) 3478–3486.
[17] J. Zhou, H. Zhang, P. Gu, J.B. Margolick, D. Yin, Y. Zhang, Breast Cancer Res. Treat. 115 (2009) 269–277.
[18] A.S. Dudkina, C.W. Lindsley, Curr. Top. Med. Chem. 7 (2007) 952–960.
[19] L.L. Simpson, A.B. Maksymowych, S. Hao, J. Biol. Chem. 276 (2001) 27034–27041.
[20] N.R. Silvaggi, D. Wilson, S. Tzipori, K.N. Allen, Biochemistry 47 (2008) 5736–5745.
[21] S. Eswaramoorthy, D. Kumaran, S. Swaminathan, Biochemistry 41 (2002) 9795–9802.
[22] M.A. Hanson, T.K. Oost, C. Sukonpan, D.H. Rich, R.C. Stevens, J. Am. Chem. Soc. 122 (2000) 11268–11269.
[23] N.R. Silvaggi, G.E. Boldt, M.S. Hixon, J.P. Kennedy, S. Tzipori, K.D. Janda, K.N. Allen, Chem. Biol. 14 (2007) 533–542.

[24] W.B. Young, P. Sprengeler, W.D. Shrader, Y. Li, R. Rai, E. Verner, T. Jenkins, P. Fatheree, A. Kolesnikov, J.W. Janc, L. Cregar, K. Elrod, B. Katz, Bioorg. Med. Chem. Lett. 16 (2006) 710–713.
[25] K.P. Yiadom, S. Muhie, D.C. Yang, Biochem. Biophys. Res. Commun. 335 (2005) 1247–1253.
[26] C.M. Guzzo, D.C. Yang, Protein Expr. Purif. 54 (2007) 166–175.
[27] J.B. Hunt, S.H. Neece, A. Ginsburg, Anal. Biochem. 146 (1985) 150–157.
[28] B.Q. Ferguson, D.C. Yang, Biochemistry 25 (1986) 529–539.
[29] B. Kramer, M. Rarey, T. Lengauer, Proteins 37 (1999) 228–241.
[30] M. Barker, M. Clackers, D.A. Demaine, D. Humphreys, M.J. Johnston, H.T. Jones, F. Pacquet, J.M. Pritchard, M. Salter, S.E. Shanahan, P.A. Skone, V.M. Vinader, I. Uings, I.M. McLay, S.J. Macdonald, J. Med. Chem. 48 (2005) 4507–4510.
[31] A. Khandelwal, V. Lukacova, D. Comez, D.M. Kroll, S. Raha, S. Balaz, J. Med. Chem. 48 (2005) 5437–5447.
[32] M.C. Holthausen, M. Mohr, W. Koch, Chem. Phys. Lett 240 (1995) 245–252.
[33] J.G. Jones, J.B. Poole, J.C. Tomkinson, R.J.P. Williams, J. Chem. Soc. (1958) 2001–2009.
[34] J.P. Gallivan, D.A. Dougherty, Proc. Natl. Acad. Sci. USA 96 (1999) 9459–9464.
[35] N. Zacharias, D.A. Dougherty, Trends Pharmacol. Sci. 23 (2002) 281–287.
[36] J.E. Zuniga, J.J. Schmidt, T. Fenn, J.C. Burnett, D. Arac, R. Gussio, R.G. Stafford, S.S. Badie, S. Bavari, A.T. Brunger, Structure 16 (2008) 1588–1597.